

Tracing sediment sources with meteoric ^{10}Be : Linking erosion and the hydrograph

Final Report: submitted June 20, 2012

PI: Patrick Belmont

Utah State University, Department of Watershed Sciences

University of Minnesota, National Center for Earth-surface Dynamics

Background and Motivation for the Study

Sediment is a natural constituent of river ecosystems. Yet, in excess quantities sediment can severely degrade water quality and aquatic ecosystem health. This problem is especially common in rivers that drain agricultural landscapes (Trimble and Crosson, 2000; Montgomery, 2007). Currently, sediment is one of the leading causes of impairment in rivers of the US and globally (USEPA, 2011; Palmer et al., 2000). Despite extraordinary efforts, sediment remains one of the most difficult nonpoint-source pollutants to quantify at the watershed scale (Walling, 1983; Langland et al., 2007; Smith et al., 2011).

Developing a predictive understanding of watershed sediment yield has proven especially difficult in low-relief landscapes. Challenges arise due to several common features of these landscapes, including a) source and sink areas are defined by very subtle topographic features that often cannot be detected even with relatively high resolution topography data (15 cm vertical uncertainty), b) humans have dramatically altered water and sediment routing processes, the effects of which are exceedingly difficult to capture in a conventional watershed hydrology/erosion model (Wilkinson and McElroy, 2007; Montgomery, 2007); and c) as sediment is routed through a river network it is actively exchanged between the channel and floodplain, a dynamic that is difficult to model at the channel network scale (Lauer and Parker, 2008). Thus, while models can be useful to understand sediment dynamics at the landscape scale and predict changes in sediment flux and water quality in response to management actions in a watershed, several key processes are difficult to constrain to a satisfactory degree. Direct measurement of erosion, deposition and sediment transport at key locations (edge of field, eroding/aggrading channel banks) are also useful and can help constrain the aforementioned models, but such efforts are costly and are inherently limited in spatial extent, sampling frequency, and level of detection (Day et al., in review).

Sediment fingerprinting is a relatively new technique that circumvents many of the key limitations of other approaches for quantifying sediment sources and understanding sediment transport at the watershed scale (see Gellis and Walling, 2011 for a complete review). When used in combination with other approaches sediment fingerprinting can provide useful information for calibrating/validating watershed models and/or upscaling local measurements of erosion and deposition. Briefly, sediment fingerprinting utilizes the geochemical composition of suspended sediment to determine the proportion derived from different parts of a watershed. The goal of this project was to develop and implement a sediment fingerprinting approach that can be used to determine the proportion of sediment derived from upland versus near-channel sources (banks and bluffs) in the Le Sueur River watershed, south-central Minnesota. It is important to note that this particular technique integrates over space and discretizes over time. For example, multiple samples collected individually over the course of a storm hydrograph provide *watershed-integrated snapshots* of the proportion of sediment derived from different

sources at each point in time throughout a storm event. This information can be used independently as a basis for determining what type of management/conservation/restoration work might be needed and for evaluating the post-project effectiveness of such work. Our sediment fingerprinting research utilized a suite of long- and short-lived radionuclide tracers (specifically, Beryllium-10 (^{10}Be) with a half-life = 1.36×10^6 years, Lead-210 (^{210}Pb) with a half-life = 22.3 years, and Cesium-137 (^{137}Cs) with a half-life = 30 years) associated with source areas and suspended sediment. The Minnesota Department of Agriculture grant supporting this work focused exclusively on the ^{10}Be results and for that reason, those results are the primary focus of this report.

Study Area

The Le Sueur River (Figure 1) drains a 2880 km² watershed and is a major source of sediment to the Minnesota and upper Mississippi rivers (Minnesota Pollution Control Agency (MPCA) et al., 2007; Engstrom et al., 2009). However, uncertainty exists regarding the relative importance of different sediment sources within the watershed. The primary potential sediment sources are bluffs (tall, cliff-like features that are typically composed of fine-grained till), ravines (steep, first- and second-order fluvial networks that connect uplands with the river valley), streambanks (fluvial features that define the river channel) and uplands (of which 92% are used for agricultural row crop production). Understanding the sediment dynamics of the current system, as well as our rationale for sample design, requires an understanding of the geomorphic organization of the system, which has been dictated largely by the geologic history of the landscape, as follows.

The south-central Minnesota landscape that comprises the Le Sueur watershed was formed over 14,000 years ago, following the retreat of the Laurentide Ice Sheet (Thorleifson, 1996). The geologic stratigraphy of the landscape includes a 60+ m thick package of interbedded fine-grained glacial tills and glacio-fluvial sediments (Jennings, 2010). Approximately 13,400 calendar years before present (11,500 radiocarbon years BP) Glacial Lake Agassiz catastrophically drained through the proto-Minnesota River Valley, incising the mainstem of the proto-Minnesota River (referred to as Glacial River Warren) over 60 m, thereby forming a knickpoint, or anomalous increase in channel gradient, near the confluence of the Le Sueur and Minnesota rivers. Since that time, the knickpoint has been migrating upstream from the mouth of the Le Sueur, creating a steep zone in the lower 40 km of the Le Sueur river network, which we refer to as the 'knick zone' (Figure 2). In the wake of the knickpoint, tall bluffs and steep, incising ravines have developed as the Le Sueur incises vertically, ultimately re-grading the river to the lower base level of the Minnesota River. Vertical incision of the river continues today at a relatively rapid pace (3-5 m/kyr; Belmont et al., 2011a).

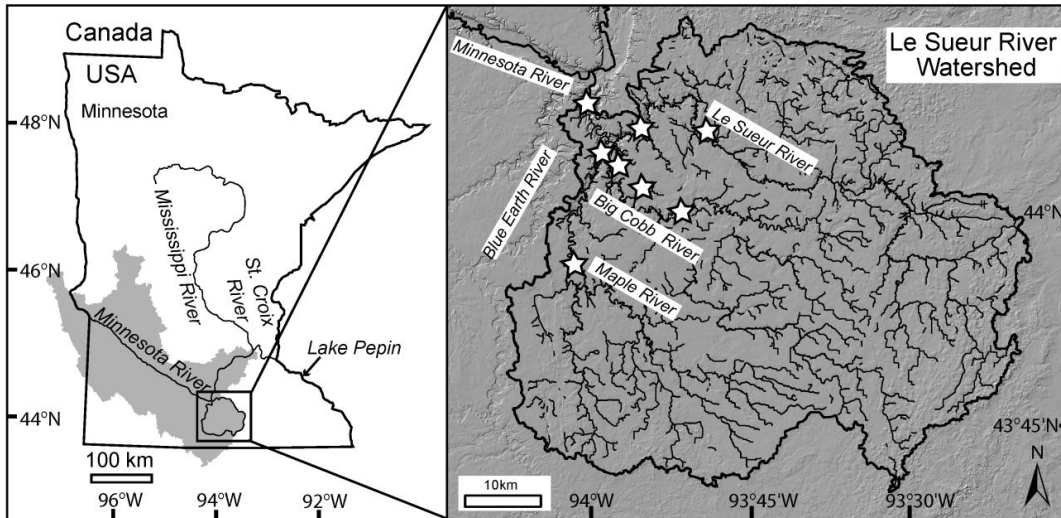


Figure 1. Location of the study area, including the Le Sueur River basin and Lake Pepin (adapted from Gran et al., 2009). Stars in right panel indicate locations of water and sediment gaging stations.

Long-term erosion estimates indicate that the Le Sueur has been a high sediment system over the past 13,400, contributing an estimated 55,000 Mg/yr to the Minnesota River on average (Gran et al., 2009; Gran et al., 2011). However, modern gaging data from the US Geological Survey and Minnesota Pollution Control Agency show that the average sediment efflux from the mouth of the Le Sueur has increased approximately four-fold, to 225,000 Mg/yr on average for the period 2000-2010 (Belmont et al., 2011b). Further, the gaging stations, which have been systematically established above and below the knickpoint on each of the three branches of the river network (see Figure 1), indicate that more than half of the sediment is contributed within the knick zone, where tall bluffs and ravines have developed, suggesting that these are substantial, and potentially dominant, sediment sources (Gran et al., 2011). Sediment fingerprinting was proposed as the focus of this study to examine the spatial and temporal patterns of sediment sources at the relatively small scale of the Le Sueur watershed and gaged sub-watersheds.

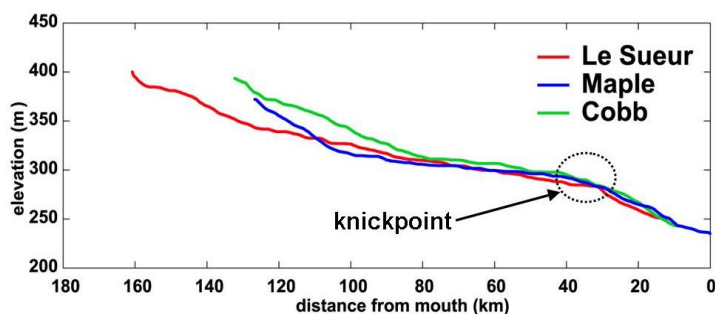


Figure 2. River longitudinal profiles indicating the elevation of the river channels with distance from the mouth of the main stem of the Le Sueur. A prominent knickpoint exists ~ 35 km from the mouth, below which the river is anomalously steep, river channels are actively incising, and large bluffs and ravines are developing.

Lake Pepin is a naturally dammed lake on the Mississippi River. Sediment cores from Lake Pepin indicate that prior to 1830, sedimentation rates in the lake were 80,000 Mg/yr on average. Since Euro-American settlement beginning in the early 19th century sedimentation rates appear

to have increased significantly to over 700,000 Mg/yr. Sedimentation rates in Lake Pepin have remained high even in recent decades, despite significant improvements in conservation and precision agriculture (Kelley et al., 2006; Musser et al., 2009). Trace mineral analysis and TSS records both suggest that the vast majority of sediment (85-90%) deposited in Lake Pepin is, and historically always has been, derived from the Minnesota River Basin (Kelley et al., 2006; Wilcock et al., 2009). The rapidly incising tributaries of the Minnesota River Basin are responsible for the relatively high sediment loads contributed prior to 1830. Less clearly understood is how the numerous and pervasive human modifications throughout the Minnesota River Basin, including vegetation clearance, artificial drainage, tillage, urban/sub-urban construction, as well as climate change, each contributed to the significant increase in sediment loading observed over the past 180 years. Geochemical fingerprinting of Lake Pepin sediment cores was proposed as part of this study to examine broad trends in sediment sources over time, at the large spatial scale of the Lake Pepin watershed.

Methods

Three general types of sediment samples were collected and analyzed for ^{10}Be within the scope of this project, referred to as Source samples, Suspended Sediment samples, and Lake Core samples. Source samples include any sediment collected directly from a source area (upland, bluff, ravine, or streambank/floodplain). Suspended sediment samples refer to Total Suspended Sediment (TSS) samples collected during or immediately following storm events from one of the gaging stations on the Le Sueur River or its tributary, the Maple River. Lake Core samples were collected from sedimentary deposits in Lake Pepin (sample material collected by previous research projects and provided for analysis within the scope of this project by Science Museum of Minnesota, St. Croix Watershed Research Station).

Throughout the course of this study, we learned that a significant amount of additional information can be obtained by utilizing a suite of three geochemical tracers, specifically Beryllium-10 (^{10}Be), Lead-210 (^{210}Pb), and Cesium-137 (^{137}Cs). Only ^{10}Be was covered under the scope of this Minnesota Department of Agriculture grant, and therefore in most cases only ^{10}Be results are interpreted. All ^{210}Pb and ^{137}Cs samples (in addition to several ^{10}Be results from outside the Le Sueur watershed) were funded by the Minnesota Pollution Control Agency and National Science Foundation. For the sake of completeness, all available results are included in this report and therefore a brief explanation of methods related to ^{210}Pb and ^{137}Cs is warranted. Beryllium-10 and ^{210}Pb are both naturally occurring isotopes that are continually produced in the atmosphere, delivered via dry deposition and/or during rain events, and adsorb tightly to soil particles within the top 5-10 and 150 cm of the soil profile for ^{210}Pb and ^{10}Be , respectively. Cesium-137 was delivered as a result of nuclear bomb testing, primarily between 1955 and 1963 (Robbins et al. 2000). The primary benefit to using this suite of tracers is that they have well constrained production rates and disparate radioactive decay rates (22.3, 30, and 1,360,000 years for ^{210}Pb , ^{137}Cs , and ^{10}Be , respectively). For more detailed discussion of sediment fingerprinting using ^{210}Pb and ^{137}Cs the reader should be directed to Schottler et al. (2010). For detailed explanation of ^{10}Be systematics the reader is directed to Willenbring and VonBlanckenburg (2010).

Meteoric ^{10}Be (hereafter referred to only as ^{10}Be) is produced in the atmosphere and delivered to Earth's surface when the atom attaches to an aerosol and is then cleansed from the atmosphere by either by dry deposition or precipitation. The rate of delivery of ^{10}Be to the soil varies by location and also over time, depending on the intensity and orientation of the geomagnetic field, atmospheric mixing, precipitation and wind patterns (Pigati and Lifton, 2004). The delivery flux has been modeled by two separate research groups using general circulation models (GCM); Field et al., (2006) uses the Goddard Institute for Space Studies Model E (GISS) and Heikkilä (2007) uses the European Centre for Medium-Range Forecasts-Hamburg Model 5 (ECHAM5). The flux predicted for southern Minnesota is consistent between the two models and exhibits low uncertainty (Willenbring and von Blanckenburg, 2010), making it a reliable fingerprinting tracer for our study area.

Once the ^{10}Be atom has been scavenged from the atmosphere and deposited on the ground, it binds tightly to soil particles within the top 1.5 m of the soil profile, exhibiting a maximum at the soil surface and exponential decrease in concentration with depth. Grain size can influence the ^{10}Be inventory of a soil because smaller particles have more surface area per unit volume or mass for ^{10}Be adsorption. Several other external factors could influence the measured concentration of ^{10}Be in the soil profile, including eolian deposition of dust particles, soil pH, and heterogeneity of soil properties. However, these were initially assumed, and within the course of this work determined, to be negligible factors for the purpose of our work in the Le Sueur watershed.

Source samples were collected by manual grab samples using a shovel or soil auger. Locations were selected systematically to represent several different parts of the watershed. Suspended sediment samples were collected at various gaging stations located throughout the watershed (see Figure 1). Approximately 20 gallons of water was collected for each sample, which was then allowed to settle several days. The sample was concentrated down to a volume of < 1 L, at which time it was freeze dried and prepared for chemical extraction of ^{10}Be and Accelerator Mass Spectrometry (AMS) analysis at Purdue University Rare Isotope Measurement (PRIME) Laboratory.

The detailed PRIME Lab protocol for meteoric ^{10}Be extraction and measurement can be obtained by emailing the lab directly. Briefly, ^{10}Be adsorbed to the sediment was removed by first leaching the sample in 0.5 M Hydrochloric acid (HCl). An elemental analysis was the performed, followed by the addition of a known mass of ^9Be (a different isotope of Beryllium that can be measured by AMS for comparison to the ^{10}Be measurement). Samples were the homogenized and dried down, then re-dissolved in a solution of Hydrofluoric (HF) acid. This step is repeated twice to ensure the complete dissolution of the sample. Next the samples were dissolved in water, with preferentially fractionates for Beryllium over other less-soluble elements. The beryllium-rich water was then dried down and subsequently purified using an ion exchange chromatography procedure. Beryllium hydroxide (BeOH) was precipitated, removed from the solution by centrifugation, dried and then oxidized over a flame to form Beryllium oxide (BeO). The BeO is pressed into cathode targets and the ratios of $^{10}\text{Be}/^9\text{Be}$ were measured using an Accelerator Mass Spectrometer (AMS). The measured ratio is used to calculate the concentration of ^{10}Be atoms per gram of sample mass (Balco, 2006) using equation 2.5, where N_{10} is the concentration of ^{10}Be (atoms/gram), M_q is the mass (grams) of the sample prior to

leaching and dissolution, R_{Be} is the measured ratio of $^{10}Be: ^9Be$, M_c is the mass (grams) of the 9Be rich carrier added to the sample, N_a is Avogadro's Number (6.022×10^{23} g/mol), n_{10} is the concentration of ^{10}Be (atoms/gram) in the carrier (typically assumed to be zero), and A_{Be} is the molar weight of Be (9.012 atoms/mol).

$$N_{10} = \left(\frac{1}{M_q} \right) * \left(\frac{(R_{Be} * M_c * N_a)}{A_{Be}} \right) - n_{10}$$

Results and Discussion

All ^{10}Be results along with analytical (AMS) uncertainty, estimates of sediment apportionment (where appropriate), as well as information regarding sample type and location information are provided in Appendix Tables 1, 2, and 3. The two end-member sources for geochemical fingerprinting with ^{10}Be are uplands and bluffs. Uplands, having been exposed to atmospheric deposition of ^{10}Be for many millennia were expected to exhibit significantly higher concentrations compared with bluffs, which have typically only been exposed to atmospheric deposition for a few years or at most, decades. Further, bluffs were expected to exhibit low levels of ^{10}Be because the high gradient that is characteristic of bluff surfaces causes foreshortening, further reducing their effective exposure to atmospheric deposition. As expected, bluff material exhibited uniformly low ^{10}Be concentrations (Figure 3).

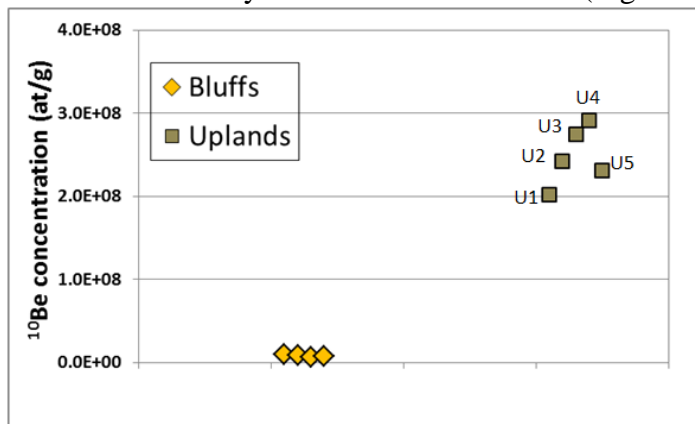


Figure 3. Beryllium-10 concentrations of end-member source areas, bluffs (yellow diamonds) and uplands (tan squares).

Upland source areas exhibit some variability, but generally fall within the range of 2 to 3E+08 atoms/gram. Variability in upland concentrations are due to a combination of differences in soil types and land use history. For example, U1 and U2 are derived from two adjacent fields that are part of the University of Minnesota Southern Research and Outreach Center in Waseca, Minnesota. Sample U1 was derived from a fallow field that has not been tilled in at least 80 years, whereas U2 was collected from a field that has been in active use for that duration. Averages for the two source areas are 0.081E+08 and 2.48E+08 atoms/gram for bluffs and uplands, respectively, indicating a 30-fold difference in concentration. These averages were used to compute sediment apportionment.

Sediment was collected from the active channel bed and point bars of the Le Sueur and Maple Rivers, sieved to $< 125 \mu\text{m}$ and analyzed for ^{10}Be . Results show a range of sediment apportionment, with a general trend toward bluff sources in the downstream direction (Figure 4).

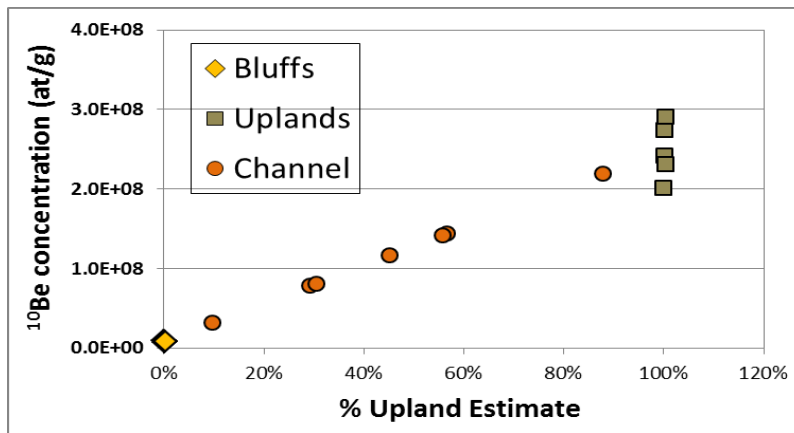


Figure 4. Beryllium-10 results from channel alluvium (bed and point bar sediment), interpreted for sediment apportionment using a two end-member unmixing model.

Samples collected from floodplains and stream banks indicate a wide range, similar to channel bed material. However, the vast majority (all but 3) of floodplain/bank samples exhibit concentrations below $1\text{E}+08$ atoms per gram, which is the equivalent of 40% upland (Figure 5). Nearly all of these samples were collected from floodplains or low terraces within the knick zone. The three samples that exhibit higher concentrations are all derived from the upper Maple River, well above the knickpoint, near county highways 7 and 46 and 225th Street in Blue Earth County.

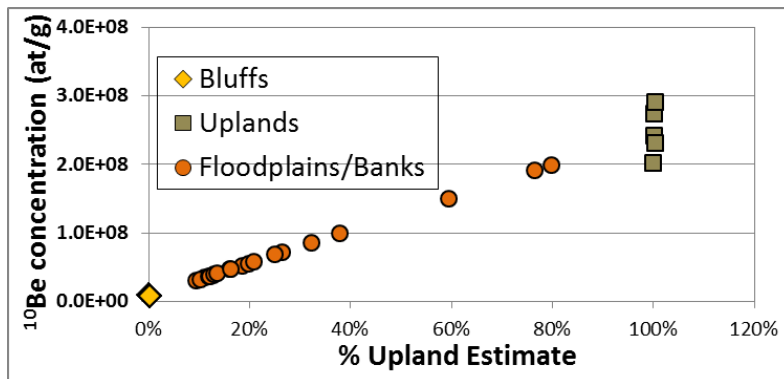


Figure 5. Beryllium-10 results from floodplains and stream banks, interpreted for sediment apportionment using a two end-member unmixing model.

These observations are consistent with the notion that floodplains record the long-term washload average for geochemical fingerprinting. Less clear at this point is the time period to which these floodplain samples are relevant. In the Le Sueur River, floodplains are constantly being constructed, reworked, and eroded with significant variability in time and space. For sediment fingerprinting purposes, the floodplains record the fingerprinting signature for the time period over which the floodplain was being constructed. Better time constraints on the floodplain material might provide additional information regarding larger shifts in sediment sources over the past few centuries. Future work should focus on further exploiting the archive of geochemical information available in the floodplains.

Samples were strategically collected from several different locations in numerous ravines, several of which are from Seven Mile Creek and are only presented in this report for context. Figure 6 shows samples plotted simply as a function of ^{10}Be concentration and sediment apportionment to demonstrate that ravine sediment can vary across nearly the full range of ^{10}Be concentrations observed between the two end-member sources. The majority of these samples were collected from fill terraces within ravines, some of which exhibit relatively low ^{10}Be concentrations (the large fill terrace in ravine 2 ranges from $5\text{E}+07$ to $7\text{E}+07$, which translates to 17-27% upland), whereas other fill terraces exhibit very high concentrations (ravine 4 fill terrace yielded sediment that exceeded the average ^{10}Be upland signature). Samples collected directly from ravine hillslopes fall within the range of $1.2\text{E}+08$ to $2.1\text{E}+08$, as expected because the ravine soil surfaces are expected to have been eroding at a rate that falls between that of the uplands and bluffs. The one TSS sample that was collected during a storm event from the lower bridge crossing at the Highway 90 ravine indicates a ^{10}Be concentration of $1.3\text{E}+08$, which would be the equivalent of 50% upland, though the assumptions of the simple two-end member unmixing model are not likely upheld for interpretation of this sample. What is clear from these data are that ravines differ somewhat from location to location in terms of the type and origin of sediment they produce. Ravines in the Le Sueur watershed do not typically contain large fill terraces. Therefore, the complication that fill terraces can contain a wide range of ^{10}Be concentrations is not a matter of concern. In Seven Mile Creek, where fill terrace samples exhibit high variability, characterization of ravines for the purpose of sediment fingerprinting would require use of more than one geochemical tracer.

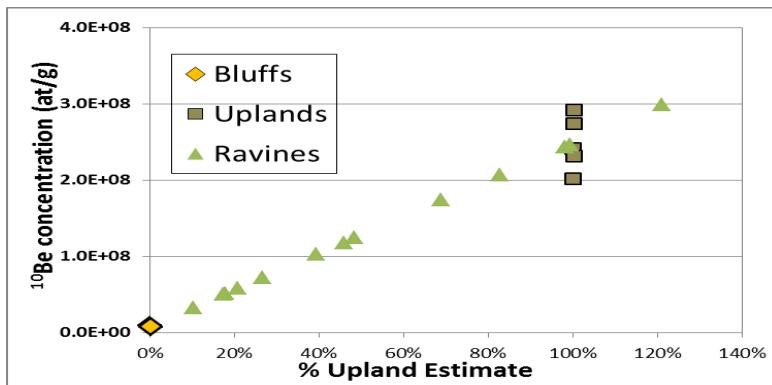


Figure 6. Beryllium-10 results from ravine samples (including hillslopes and fill terraces within ravines), interpreted for sediment apportionment using a two end-member unmixing model.

The ^{10}Be concentration in a suspended sediment sample reflects the proportion of sediment derived from different sources at a particular point in time. Figure 7 shows all TSS samples analyzed for ^{10}Be in terms of concentration as well as sediment apportionment (percent of sediment derived from upland sources). Blue circles indicate samples collected at gages above the knickpoint (specifically, at the upper gage on the Le Sueur River in St. Clair, Minnesota and the upper gage on the Maple River at Blue Earth County highway 18). Red circles indicate samples collected at gages within the knick zone (specifically, the Le Sueur gages at Red Jacket Park and Blue Earth County highway 8 as well as the lower Maple River gage at Blue Earth County highway 35). While there is overlap between the two populations, there is a general shift to lower concentrations at the lower gages, as expected from a higher proportion of bluff inputs within the knick zone.

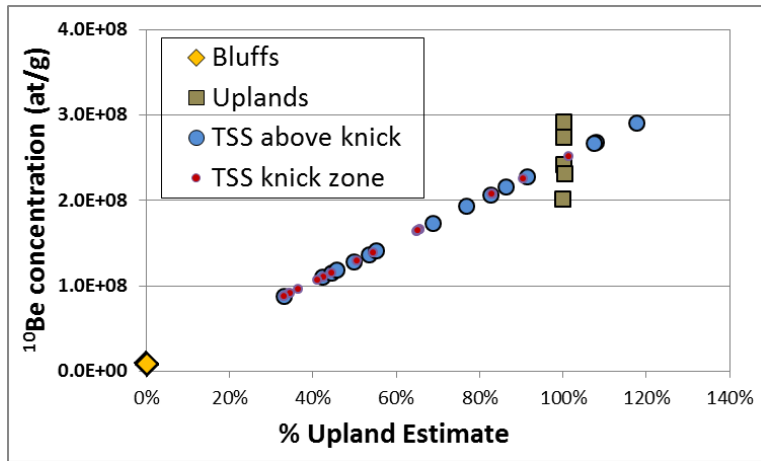


Figure 7. Beryllium-10 results from TSS samples collected at gaging stations above the knickpoint (blue dots, including upper Le Sueur gage in St. Clair, MN and upper Maple River gage at Hwy 18) and within the knick zone (red dots, including Le Sueur gages at Red Jacket Park and Highway 8 as well as the lower Maple River gage at Highway 35) interpreted for sediment apportionment using a two end-member unmixing model.

One of the goals of this project was to demonstrate whether or not ^{10}Be can be used to demonstrate shifts in sediment sources over the course of individual storm hydrographs. Because the floodplains/banks exhibit ^{10}Be concentrations that fall between the two end-member sources we are unable to differentiate between upland, bluffs, and banks individually using ^{10}Be alone. However, ^{10}Be concentrations can be used in combination with measurements of a short-lived radionuclide to differentiate inputs from stream banks.

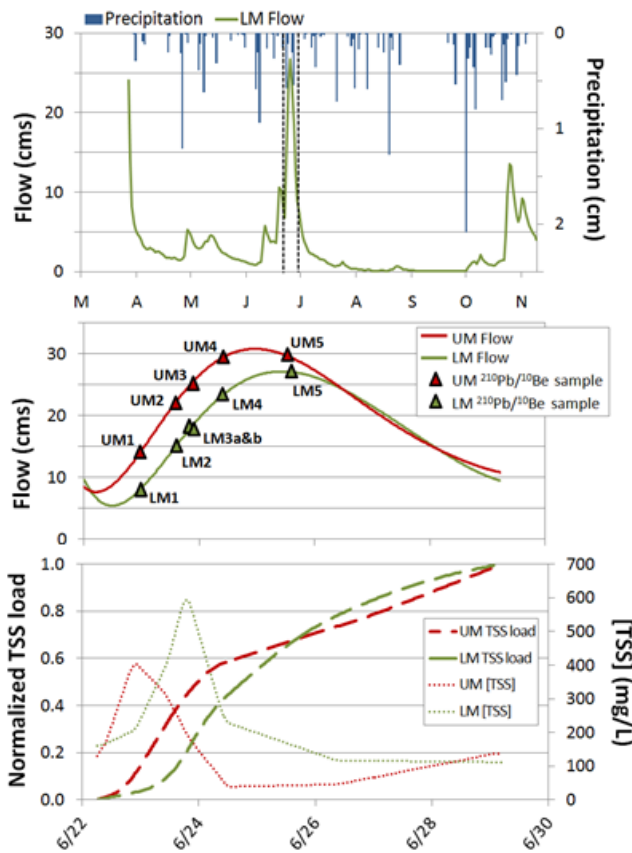


Figure 8. Top panel shows precipitation (blue bars, right axis) and annual hydrograph (green line, left axis) for the 2009 sampling season at the Lower Maple River gaging station located at Blue Earth County highway 35. Middle panel shows hydrographs for upper and lower Maple River gages (red and green lines, respectively) and timing of sample collection for the June 2009 event. Lower panel shows measured TSS concentrations and cumulative load over the course of the event (dotted and dashed lines, respectively).

We collected a complete set of samples from the upper and lower Maple River gages (referred to as UM and LM, respectively) during the largest storm event of 2009. Figure 8 shows the magnitude of the event within the context of the annual hydrograph, the timing of sample collection at each gage (including a pair of field replicates collected at the lower Maple gage (LM3a&b)), and the TSS concentrations (also shown as cumulative loads) measured by the Water Resource Center over the course of the event. Figure 9 shows the ^{210}Pb activity and ^{10}Be concentrations for each of the samples. It is noteworthy that the relatively simple unmixing model we have applied provides reasonable numbers that are consistent with our geomorphic understanding of the system. Above the UM gage, uplands are essentially the only source that can contribute sediment, consistent with measured ^{10}Be concentrations for suspended sediment collected at the UM gage (shown in red) that are very similar to concentrations measured for our upland source. Two UM samples are interpreted for sediment apportionment as >100% upland, which could be caused by additional ^{10}Be delivery to floodplain alluvium during storage and/or a slight underestimate of our upland source fingerprint. The systematic decrease in ^{10}Be concentrations observed between the UM and LM gages is consistent with the observation that the frequency of bluffs increases significantly between the gages, as the river enters the incising knick zone.

The short-lived radionuclide (^{210}Pb) exhibits systematically lower (normalized) concentrations than ^{10}Be , with one exception (UM 4), which is likely caused by a sample processing error (loss of ^{10}Be during column chemistry). Disparity between the long- and short-lived radionuclide source apportionment estimates is a measure of floodplain/bank contributions.

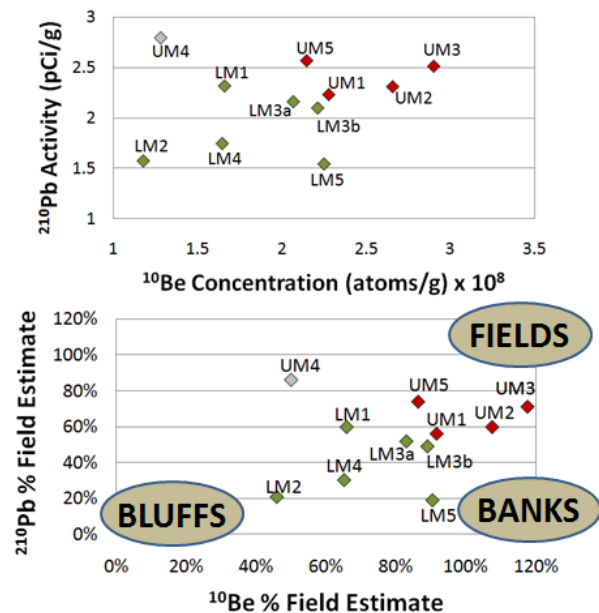


Figure 9. Top panel shows radionuclide results (^{210}Pb reported as an activity level and ^{10}Be reported as concentration). Bottom panel plots both radionuclide results in terms of sediment apportionment.

While much variability exists in soil type, climate, and land use history throughout the Minnesota River Basin, all of the Minnesota tributaries have a relatively similar geomorphic structure (low-gradient agricultural ditches, low-gradient natural channels above the knickpoint, and high gradient natural channels within the knick zone). While land use history varies

throughout the Minnesota River Basin, the general shift from forest/wetland/prairie to agriculture is pervasive. It is therefore conceivable that the effects of changes in these large scale drivers might be recorded in the Lake Pepin sedimentary record. When evaluating sediment transport through large river systems, such as the Minnesota and upper Mississippi rivers, sediment storage is an important consideration. The glacial flood events that incised the Minnesota River Valley greatly reduced the slope, and therefore the transport capacity, of the Minnesota River (Belmont et al., 2011). Grain size distributions in Lake Pepin cores are comprised almost exclusively of silt and clay, indicating that all sand and gravel contributed from incising MRB tributaries is stored upstream from Lake Pepin. Further, analysis of TSS data indicates 25-50% storage of TSS between the gages at Judson and Fort Snelling in the lower Minnesota River (Wilcock et al., 2009). So the relationship between sediment contributions throughout the watershed and sediment delivery to Lake Pepin is clearly a complicated one, further emphasizing the need for multiple approaches to quantify and predict sediment dynamics of the system.

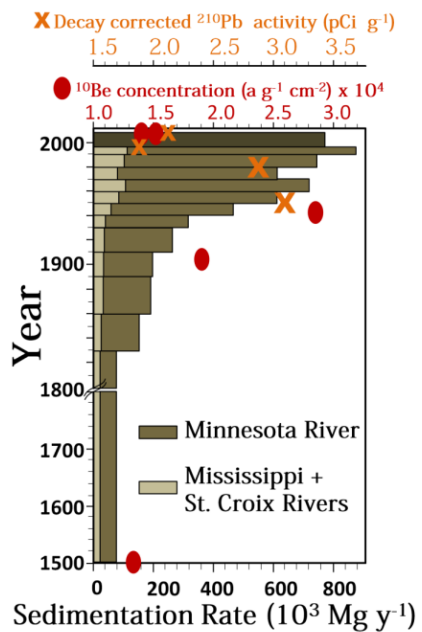


Figure 10. Figure taken from Belmont et al., 2011. Depth profile of Lake Pepin sedimentary record showing sedimentation rate (bottom axis) and concentrations of radionuclide sediment tracers (top axes).

We analyzed ^{210}Pb and ^{10}Be in Lake Pepin sediment cores to document the relative proportion of fine sediment derived from uplands versus near-channel sources over the past 500 years. Both tracers show similar changes over time (Figure 10, red dots for ^{10}Be , orange Xs for ^{210}Pb). The low ^{10}Be concentration measured in sediment delivered to Lake Pepin 500 years ago indicates very little upland soil erosion relative to bluff erosion at that time. During the mid-1900s, an increase in ^{10}Be concentrations indicates a pulse of soil erosion from agricultural fields, presumably as a result of enhanced capacity for soil disturbance and poor conservation practices. Over the past three decades, both tracers indicate shifts back toward near-channel sources. The interpretation of this trend is that upland soil erosion may have declined in response to the emergence of precision-agriculture practices and enhanced conservation efforts. But any reduction in sediment inputs from these activities has been offset by an increase in near-channel erosion, resulting from dramatic increases in high flows, documented by Novotny and Stefan, (2007) among others. This shift in sources is further supported by the sediment budget developed at the much smaller scale of the Le Sueur watershed which uses multiple lines of

information to pinpoint near-channel erosion as the dominant source during the time period 2000 to 2010 (Belmont et al., 2011b).

Appendix Table 1. Beryllium-10 results for end-member source areas and ravines

Sample ID	Sample Type	10Be conc (at/g)	AMS Uncertainty	% Upland Est.	UTM Easting	UTM Northing	Notes
B09Vii1C	bluff	9.11E+06	3%		429402	4887040	Le Sueur hwy 83. 3m above toe, 60m up from bluff
B09vii1F	bluff	8.92E+06	3%		423091	4880957	Le Sueur hwy 15, CR 178. 5m above culvert, 10m from road, tributary
B09Vii1D	bluff	6.78E+06	4%		429436	4887058	Le Sueur hwy 83. 75m up from bridge, 4m above toe
B09Vii1E	bluff	7.71E+06	3%		423049	4880936	Le Sueur hwy 15, CR 178. 4m above culvert bottom, 20m from road, tributary
S09Viii28B	upland - field	2.02E+08	1%		458360	4878849	Hwy 14, Waseca. Soybean ag. field. Flat, tilled and other crops separated by road. 0 - 10 cm deep
S09Viii28A	upland - non-field	2.42E+08	2%		457907	4880721	Hwy 14, Waseca. lawn w/ large trees 5 - 20 m tall. Oak trees 100+ years old. Grass, clover, and shrubs. Weeds. Multiple samples 2 -20 cm deep.
S09viii7A	upland - field	2.74E+08	2%				Hwy 90 test site. samples #1 - 8
S09Viii7C	upland - field	2.91E+08	3%				Hwy 90 test site. samples #17 - 24
S09vii28J	upland- field	2.31E+08	3%				SMI Creek. Row crop upland.
S09Vii28E	ravine	5.08E+07	2%	18%			ravine fill terrace 1.5m from top
S09Vii29C	ravine	1.73E+08	1%	69%	415270	4901490	ravine 3 hillcrest, med/lg trees, many downed, 1.5m from top
S09vii28L	ravine	7.19E+07	2%	27%	416444	4902460	ravine 2 fill terrace bottom 1.5m from bottom
S09vii28M	ravine	4.96E+07	1%	17%			ravine 2 fill terrace, 3 m from bottom
S09vii28K	ravine	5.76E+07	2%	21%			ravine 2 fill terrace, 0.5m from top
S09vii28G	ravine	2.43E+08	2%	98%			ravine fill terrace
S09vii28D	ravine	3.24E+07	2%	10%			ravine fill terrace 30cm from top
S09Vii28I	ravine	2.98E+08	1%	121%			ravine 4 fill terrace bottom 1.5m up
S09Vii28A	ravine	2.07E+08	2%	83%	416642	4901450	Composite of samples collected from bottoms of ravine gullies along the hillslope of ravine.
S09Vii28B	ravine	1.18E+08	2%	46%	416642	4901450	Composite of samples collected from tops of ravine along the hillslope of ravine.
S09Vii28C	ravine	1.24E+08	3%	48%	416638	4901548	Small fill terrace in ravine. Mostly fine grained sand and silt, organic rich.
S09Vii28F	ravine	1.02E+08	3%	39%	416651	4901792	4 m thick fill terrace in ravine. Bottom-most layer (of 3 total), ~ 3m below surface and 1 m above channel bed.
S09Vii28G	ravine	2.47E+08	3%	99%	416651	4901792	4 m thick fill terrace in ravine. Middle layer (of 3 total), ~ 1.5m below terrace surface.

Appendix Table 2. Beryllium-10 results for channel and floodplain samples

Sample ID	Sample Type	10Be conc (at/g)	AMS Uncertainty	% Upland Est.	UTM Easting	UTM Northing	Notes
S08Vii10MF	channel	1.44E+08	2%	57%	431818	4849694	County Road 21 Channel alluvium.
S08Vii10MG	channel	2.19E+08	1%	88%	431818	4849694	County Road 21 Channel alluvium, bank.
S08Vii10MJ	channel	1.42E+08	5%	56%	424376	4855218	Maple River near Hwy 46, channel alluvium.
S08Vii10MK	channel	7.80E+07	2%	29%	424376	4855218	Maple River near Hwy 46, channel alluvium.
S08Vii10MN	channel	1.16E+08	2%	45%	422864	4858356	Maple River near Hwy 7, bar sample
S08Vii10MP	channel	8.14E+07	2%	31%	422864	4858356	Maple River near Hwy 7, bed alluvium sample. Le Sueur hwy 8, immediately downstream from bridge. Mud mantle in channel.
S09iV19LC	channel	3.15E+07	2%	10%			
S08Vii10MI	bank/floodplain	1.51E+08	6%	59%	427670	4851113	Maple River near 225th Street, bank material. Maple River near Hwy 46, upland/floodplain grab sample.
S08Vii10ML	bank/floodplain	1.91E+08	2%	76%	424376	4855218	
S08Vii10MO	bank/floodplain	2.00E+08	2%	80%	422864	4858356	Maple River near Hwy 7, bank sample
S08Vii10MQ	bank/floodplain	9.88E+07	2%	38%	416431	4861894	Maple River near Hwy 30, bank sample.
S08Vii10MT	bank/floodplain	7.15E+07	2%	26%	414077	4864993	Maple River near Hwy 18, bank sample.
S10X05A	bank/floodplain	3.04E+07	3%	9%			Channel deposit of mud at Red Jacket, following severe Sept 2010 flood.
S10X05B	bank/floodplain	3.44E+07	3%	11%			Floodplain mud deposit from Sept 2010 flood, collected ~ 150 m downstream from St. Clair gage.
S10X05C	bank/floodplain	3.27E+07	2%	10%			Floodplain mud deposit from Sept 2010 flood, collected from right floodplain in Wildwood Park.
S10Xi18A	bank/floodplain	5.27E+07	5%	19%	430629	4886277	Wildwood park low terrace sample on Le Sueur River. Zero to 29" (73 cm) depth.
S10Xi18B	bank/floodplain	3.88E+07	8%	13%	430629	4886277	Wildwood park low terrace sample on Le Sueur River. 29-58" (73-147 cm) depth.
S10Xi18C	bank/floodplain	3.65E+07	3%	12%	430629	4886277	Wildwood park low terrace sample on Le Sueur River. 58-88" (147-223 cm) depth.
S10Xi19A	bank/floodplain	3.69E+07	2%	12%	430654	4886251	Wildwood park floodplain sample on Le Sueur River. Zero to 15" (39 cm) depth.
S10Xi19B	bank/floodplain	5.54E+07	2%	20%	430654	4886251	Wildwood park floodplain sample on Le Sueur River. 15-31" (39-79 cm) depth.
S10Xi19C	bank/floodplain	5.81E+07	2%	21%	430654	4886251	Wildwood park floodplain sample on Le Sueur River. 31-82" (79-208 cm) depth.
S10Xi20A	bank/floodplain	6.82E+07	4%	25%	419158	4881218	terrace just downstream from hwy 16 bluff on Le Sueur River, on river left just after bend. Zero to 26" (66 cm) of actual core. Dark to light transition in sediment color.
S10Xi20B	bank/floodplain	8.52E+07	2%	32%	419158	4881218	terrace just downstream from hwy 16 bluff on Le Sueur River, on river left just after bend. 26-42" (66-107 cm) depth of actual core. Dark sediment color.
S10Xi20C	bank/floodplain	4.66E+07	2%	16%	419158	4881218	terrace just downstream from hwy 16 bluff on Le Sueur River, on river left just after bend. 42-76" (107-193 cm) depth. Light sediment color.
S10Xi20D	bank/floodplain	3.93E+07	2%	13%	419140	4881231	floodplain just below terrace sampled S10xi20A-B-C, just downstream from hwy 16. Zero to 30" (76 cm) depth.
S10Xi20E	bank/floodplain	4.06E+07	2%	14%	419140	4881231	floodplain just below terrace sampled S10xi20A-B-C, just downstream from hwy 16. 30-60" (76-152 cm) depth
S10Xi20F	bank/floodplain	4.69E+07	2%	16%	419140	4881231	floodplain just below terrace sampled S10xi20A-B-C, just downstream from hwy 16. 60-86" (152-218 cm) depth.

Appendix Table 3. Beryllium-10 results for TSS samples

Sample ID	Sample Type	10Be conc (at/g)	AMS Uncertainty	% Upland Est.	Notes
W09Vi23A	water	1.66E+08	3%	66%	13:00 Le Sueur mouth, Red Jacket Park
S10iX27B	water	1.10E+08	1%	43%	13:15 Le Sueur mouth, Red Jacket Park
S10X05A	water	9.59E+07	1%	37%	13:00 Le Sueur mouth, Red Jacket Park
W09Vi23H	water	1.15E+08	3%	45%	14:30 Le Sueur River at Hwy 8
W09Viii19A	water	1.39E+08	4%	55%	13:40 Le Sueur River at Hwy 8
W09Vi23H	water	2.51E+08	1%	101%	14:30 Le Sueur River at Hwy 8
S10iX24B	water	1.30E+08	2%	51%	12:35 Le Sueur River at Hwy 8
S10iX27A	water	9.06E+07	2%	34%	12:45 Le Sueur River at Hwy 8
S10X03A	water	1.07E+08	1%	41%	11:50 Le Sueur River at Hwy 8
W09Vi23C	water	1.36E+08	2%	53%	15:20 Le Sueur River at St. Clair, upper Le Sueur
W09Viii19B	water	1.10E+08	2%	42%	14:00 Le Sueur River at St. Clair, upper Le Sueur
W09Vi23S	water	1.41E+08	2%	55%	14:50 Le Sueur River at St. Clair, upper Le Sueur
W09Viii20A	water	1.15E+08	2%	45%	13:10 Le Sueur River at St. Clair, upper Le Sueur
S10iX24A	water	2.67E+08	1%	108%	10:30 Le Sueur River at St. Clair, upper Le Sueur
S10X05D	water	8.77E+07	2%	33%	18:00 Le Sueur River at St. Clair, upper Le Sueur
W09Vi23L	water	1.24E+08	2%	48%	15:20 Hwy 90 ravine on Le Sueur River.
W09Vi23AD	water	1.29E+08	2%	51%	15:20 Hwy 90 ravine on Le Sueur River.
W09Vi23AA	water	2.90E+08	3%	118%	21:00 Upper Maple River gage at hwy 18.
W09Vi22A	water	2.28E+08	3%	92%	23:00 Upper Maple River gage at hwy 18.
W09Vi23B	water	2.66E+08	2%	108%	14:00 Upper Maple River gage at hwy 18.
W09Vi24B	water	1.28E+08	3%	50%	9:50 Upper Maple River gage at hwy 18.
W09Vi30A	water	2.06E+08	2%	83%	14:40 Upper Maple River gage at hwy 18.
W09Vi23B*	water	1.18E+08	5%	46%	14:00 Upper Maple River gage at hwy 18.
W09Viii19D	water	1.73E+08	2%	69%	15:00 Upper Maple River gage at hwy 18.
W09Viii20D	water	1.93E+08	4%	77%	14:30 Upper Maple River gage at hwy 18.
W09Vi25A	water	2.15E+08	3%	86%	12:50 Upper Maple River gage at hwy 18.
W09Vi23AB	water	2.07E+08	2%	83%	20:15 Lower Maple River gage at hwy 35.
W09Vi30B	water	2.07E+08	3%	83%	15:45 Lower Maple River gage at hwy 35.
W09Vi22B I	water	1.66E+08	3%	66%	23:30 Lower Maple River gage at hwy 35.
W09Vi24A I	water	1.64E+08	4%	65%	9:30 Lower Maple River gage at hwy 35.
W09Vi24A II	water	1.65E+08	2%	65%	9:30 Lower Maple River gage at hwy 35.
W09Vi25B	water	2.25E+08	1%	90%	14:15 Lower Maple River gage at hwy 35.
S10X02A	water	9.12E+07	1%	35%	14:00 Lower Maple River gage at hwy 35.
S10X05B	water	8.75E+07	4%	33%	14:00 Lower Maple River gage at hwy 35.
Lake Pepin I.	lake sediment	1.44E+08	4%		surface
Pepin IV.4_2c	lake sediment	2.53E+08	3%		surface
Pepin IV.4_9c	lake sediment	4.81E+08	2%		1940
Pepin IV.4_1c	lake sediment	3.14E+08	3%		1890
Pepin IV.4_1f	lake sediment	2.25E+08	2%		1500

References

Belmont, P. Floodplain width adjustments in response to rapid base level fall and knickpoint migration. *Geomorphology* 2011, 128, 92–102.

Belmont, P.; Gran, K. B.; Jennings, C.; Wittkop, C. Holocene Landscape Evolution and Erosional Processes in the Le Sueur River, Central Minnesota. Kirk Bryan Field Trip Guide for 2011 Geological Society of America Annual Meeting. 2011a.

Belmont, P., Gran, K.B., Schottler, S.P., Wilcock, P.R., Day, S.S., Jennings, C., Lauer, J.W., Viparelli, E., Willenbring, J.K., Engstrom, D.R., Parker, G. Large shift in source of fine sediment in the Upper Mississippi River. *Environmental Science and Technology*. (2011b) 45, 8804–8810.

Day, S.S., Gran, K.B., Belmont, P., Wawrzyniec T. (in review) Pairing Aerial Photographs and Terrestrial Laser Scanning to Create a Watershed Scale Sediment Budget. submitted to *Earth Surface Processes and Landforms*.

Engstrom, D. R.; Almendinger, J. E.; Wolin, J. A. Historical changes in sediment and phosphorus loading to the upper Mississippi River: mass-balance reconstructions from the sediments of Lake Pepin. *J. Paleolimnol.* (2009) 41, 563–588.

Field, C.V., Schmidt, G.A., Koch, D., Salyk, C., Modeling production and climate related impacts on ^{10}Be concentration in ice cores. *Journal of Geophysical Research* (2006) 111, D15107. doi:10.1029/2005JD006410.

Gran, K. B.; et al. Management and restoration of fluvial systems with broad historical changes and human impacts. *GSA Sp. Paper* (2009) 451, 119–130.

Gran K.B. et al. An Integrated Sediment Budget for the Le Sueur River, southern Minnesota. Final Report submitted to Minnesota Pollution Control Agency May 2011.

Gellis, A.C., Walling, D.E. Sediment Source Fingerprinting (Tracing) and Sediment Budgets as Tools in Targeting River and Watershed Restoration Programs. in *Stream Restoration in Dynamic Fluvial Systems: Scientific Approaches, Analyses, and Tools*. Geophysical Monograph Series 194. American Geophysical Union. (2011) doi: 10.1029/2010GM000960

Heikkilä, U. Modeling of the atmospheric transport of the cosmogenic radionuclides ^{10}Be and ^7Be using the ECHAM5-HAM General Circulation Model. Ph.D. thesis. (2007) ETH-Zurich. 148 pp.

Jennings, C. E. Open File Report 10-03, Minnesota Geological Survey, map, report and digital files. 2010. ftp://mgssun6.mngs.umn.edu/pub4/ofr10_03/

Kelley, D. W.; Brachfeld, S. A.; Nater, E. A.; Wright, H. E., Jr. Historical changes in sediment and phosphorus loading to the upper Mississippi River: mass-balance reconstructions from the sediments of Lake Pepin. *J. Paleolimnol.* (2006) 35, 193–206.

Langland, M. J.; Moyer, D. L.; Blomquist, J. Changes in streamflow, concentrations, and loads in selected non-tidal basins in the Chesapeake Bay Watershed, 1985_2006. U.S. Geol. Surv. Open File Rep. (2007), 1372, 76.

Lauer, J. W.; Parker, G. Modeling framework for sediment deposition, storage, and evacuation in the floodplain of a meandering river, Part I: Theory. *Water Resour. Res.* (2008) 44, W04425.

Montgomery, D. R. Soil erosion and agricultural sustainability. *Proc. Natl. Acad. Sci.* (2007) 104, 13268–13272.

Musser, K.; Kudelka, S.; Moore, R. Minnesota River Basin Trends Report. 2009; 66 pp.
<http://mrbdc.wrc.mnsu.edu/mnbasin/trends/index.html>

Novotny, E. V.; Stefan, H. G. Stream flow in Minnesota: Indicator of climate change? *J. Hydrol.* (2007) 334, 319–333.

Palmer, M. A.; et al. Linkages between aquatic sediment biota and life above sediments as potential drivers of biodiversity and ecological processes. *BioScience* (2000) 50, 1062–1075.

Pigati, J.S., Lifton, N.A. Geomagnetic effects on time-integrated cosmogenic nuclide production with emphasis on in situ ¹⁴C and ¹⁰Be. *Earth and Planetary Science Letters* 226 (2004) 193– 205.

Schottler, S. P.; Engstrom, D. R.; Blumentritt, D. Fingerprinting sources of sediment in large agricultural river systems. Report for MPCA. 2010. <http://www.smm.org/static/science/pdf/scwrs-2010fingerprinting.pdf>

Smith, S. M. C.; Belmont, P.; Wilcock, P. R. Closing the gap between watershed modeling, sediment budgeting, and stream restoration. In *Stream Restoration in Dynamic Systems: Scientific Approaches, Analyses, and Tools*. Simon, A., Bennett, S. J., Castro, J., Thorne, C., Eds.; AGU: Washington, D. C., 2011 (doi:10.1029/2011GM001085).

Thorleifson, L.H., 1996. Review of Lake Agassiz history. In: Teller, J.T., Thorleifson, L.H., Matile, G., Brisbin, W.C. (Eds.), *Sedimentology, geomorphology and history of the central Lake Agassiz basin: Geological Association of Canada/Mineralogical Association of Canada Annual Meeting, Winnipeg, Manitoba, 27-29 May 1996: Field Trip Guidebook, B2*, pp. 55–84.

Trimble, S. W.; Crosson, P. U.S. Soil Erosion Rates, Myth and Reality. *Science* (2000), 289, 248–250.

US Environmental Protection Agency. Water Quality Assessment and TMDL Information. 2011.
http://iaspub.epa.gov/waters10/attains_nation_cy.control

Walling, D. E. The sediment delivery problem. *J. Hydrol.* (1983) 65, 209–37.

Wilcock, P. (2009) Synthesis Report for Minnesota River Sediment Colloquium. Report for MPCA.
http://www.lakepepinlegacyalliance.org/SedSynth_FinalDraft-formatted.pdf

Wilkinson, B.H. and McElroy, B.J., The impact of humans on continental erosion and sedimentation. *Geological Society of America Bulletin*, (2007), 119(1): 140-156.

Willenbring, J. K.; von Blanckenburg, F. Meteoric cosmogenic Beryllium-10 adsorbed to river sediment and soil: applications for Earth-surface dynamics. *Earth Sci. Rev.* (2010), 98, 105–122.